Research Article

Synthesis, spectroscopic characterization, XRD crystal structure, DFT and antimicrobial study of (2E)-3-(2,6-dichlorophenyl)-1-(4-methoxyphenyl)-prop-2-en-1-one

Nutan V. Sadgir[1] · Sunil L. Dhonnar[1] · Bapu S. Jagdale[2] · Arunkumar B. Sawant[3]

Received: 25 March 2020 / Accepted: 15 May 2020 / Published online: 15 July 2020
© Springer Nature Switzerland AG 2020

Abstract
The single crystal of synthesized (2E)-3-(2, 6-dichlorophenyl)-1-(4-methoxyphenyl) prop-2-en-1-one is characterized by FT-IR, UV–visible, ^{1}H NMR, HRMS techniques. The molecular structure was elucidated by using single-crystal X-ray diffraction technique. The title compound crystallizes in the orthorhombic crystal system of P-2_1 2_1 2_1 space group where the unit cell parameters are a = 6.4704 (4) Å, b = 12.9304 (8) Å, c = 16.7181 (11) Å, α = 90°, β = 90°, γ = 90° and Z = 4. The molecular geometry, vibrational frequencies (FT-IR) of title compound have been calculated using the DFT/(B3LYP) method with 6-311++ G (d, p) basis set and compared with the experimental data which shows good agreement. TD-DFT approach is used to compute the UV–visible spectrum. The HOMO–LUMO energy gap, experimentally (4.1096) and theoretically calculated (4.09096) are nearly same. The chemical reactivity parameters have also been studied. The results obtained from the DFT analysis show good agreement with experimental data. The synthesized compound was also screened for antimicrobial activity and it shows moderate antimicrobial activity.

Graphic abstract (2E)-3-(2,6-dichlorophenyl)-1-(4-methoxyphenyl)prop-2-en-1-one is prepared and characterize with single crystal diffraction technique. The properties were theoretically and experimentally studied and results show good agreement. Synthesized compound possesses moderate antimicrobial activity against selected pathogens for study.

✉ Nutan V. Sadgir, nutansadgir@gmail.com | [1]Department of Chemistry, L.V.H. Arts, Science and Commerce College, Panchavati, Nashik, M.S, India. [2]Department of Chemistry, Arts, Science and Commerce College, Manmad, Dist.-Nashik, M.S, India. [3]Department of Chemistry, M.S.G. Arts, Science and Commerce College, Malegaon Camp, Dist.-Nashik, M.S, India.

SN Applied Sciences (2020) 2:1376 | https://doi.org/10.1007/s42452-020-2923-9

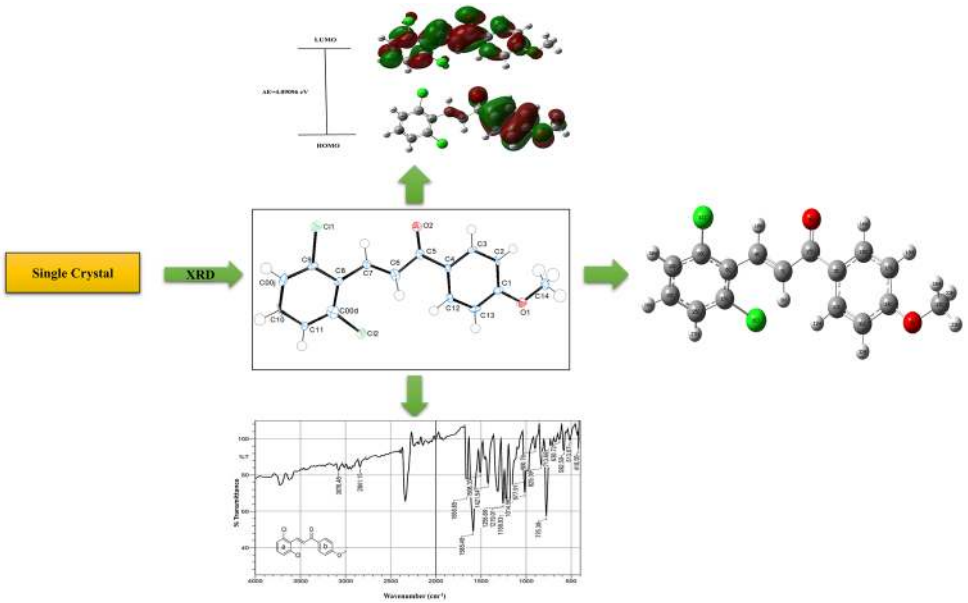

Keywords DFT · Chalcone · XRD · FT-IR · HOMO–LUMO

1 Introduction

Chalcones are open-chain Flavonoids in which the two aromatic rings are joined by a three-carbon chain [1]. They display a wide range of pharmacological properties, such as antibacterial [2], antifungal [3], antimutagenic [4], antimitotic and antiproliferative [5], antitumor [6], antioxidant [7], anti-inflammatory [8], antimalarial [9, 10], antileishmanial activity [10], antitubercular [11] and anti-diabetic [12]. Chalcones have attracted much attention for past decades due to the application as marine biofouling preventing agent [13], fluorescent probes [14] as conductive organic solar cells [15] and sweetening agent [16]. They are also useful in materials science fields such as nonlinear optics [17], optoelectronics [18], electrochemical sensing [19], Langmuir films and photoinitiated polymerization [20]. Because of the significant applications of chalcones here, we report the crystal structure of (2E)-3-(2, 6-dichlorophenyl)-1-(4-methoxyphenyl) prop-2-en-1-one. The compound was crystallized and its final structures were confirmed after diffracting this on single-crystal X-ray diffractometer. Along with this, we also report a combined experimental and theoretical analysis of molecular structure, vibrational and electronic spectra of the title compound. For the theoretical analysis of the title compound, density functional theory (DFT) calculations have been performed at B3LYP functional and 6-311++ G (d, p) basic set combination. The TD-DFT procedure is used to compute UV–visible spectral properties. In addition to this, the FMOs, electronic transition, global chemical reactivity descriptors are studied. The title molecule screened for antimicrobial activity.

2 Experimental

2.1 Material and physical measurement

The melting point is determined in open capillaries and is uncorrected. The purity of the compound was checked by TLC using silica gel-G coated Aluminum plates and spot visualize under UV radiation. FT-IR spectrum was recorded on Shimadzu spectrometer using KBr pellets. ^{1}H NMR spectrum was recorded on a Brucker Avance II 500 MHz spectrometer using TMS as an Internal Standard. The electronic absorption spectrum of the title compound was recorded at room temperature in dichloromethane solution on a Shimadzu UV–Vis spectrometer working at 200–800 nm. High-resolution mass spectrometry analysis was conducted by using the ESI mode on Bruker Impact II UHR-TOF MS instrument.

2.2 Synthesis and crystal growth

Synthesis of (2E)-3-(2, 6-dichlorophenyl)-1-(4-methoxyphenyl) prop-2-en-1-one A mixture of 4-methoxy acetophenone (1 mol) and 2, 6-dichlorobenzaldehyde (1 mol.) was dissolved in ethanol (15–20 mL) and 5 mL of KOH (20%) was added to the solution dropwise with stirring at room temperature and continue the stirring further for 4 h. The obtained product was filtered, washed with water, dried and recrystallized from ethanol. Crystals suitable for X-ray diffraction study were obtained by a slow evaporation technique using ethanol as solvent.

Yield: 92%; melting point: 182 °C; UV–Vis (λ_{Max}, nm, dichloromethane): 308; FT-IR (KBr, cm^{-1}): 3076 (aromatic C–H), 2841 (C–H), 1656 (C=O), 1585 (C=C) 1508 (aromatic C=C), 713 (C–Cl); ^{1}H NMR (500 MHz, $CDCl_3$, δ/ppm): 8.04 (d, 2H, J = 7.5 Hz), 7.85 (d, 1H, J = 15.6 Hz), 7.68 (d, 1H, J = 15.6 Hz), 7.39 (d, 2H, *J* = 8 Hz), 7.23(t, 1H, J = 8 Hz), 6.9 (d, 2H, J = 7.5 Hz), 3.82 (s, 3H); calculated mass (m/z) for $C_{16}H_{12}O_2Cl_2$:307.0292 $[M+H]^+$; HR-MS (m/z): 307.0287 $[M+H]^+$ (Scheme 1).

2.3 X-ray data collection and refinement

The single crystal XRD data were collected on a Bruker D8 Venture diffractometer. Measurements were performed at 273 (2) K temperature using graphite monochromatic Cu-K_α radiation (λ = 1.54178 Å). The crystal structure was solved by using direct methods of SHELXS-14/5 and refined by full-matrix least-squares refinement methods based on F2 with SHELXL-17/1 program [21]. All non-hydrogen atoms were refined anisotropically. The molecular graphics were drawn using Ortep-3 programs [22]. The crystallographic data and refinement parameters are given in Table 1 and a selection of bond lengths and angles are shown in Table 2.

2.4 Computational details

The DFT calculations were performed using Gaussian W (03) program package [23]. The molecular geometries were optimized in the ground state by using B3LYP [24, 25] exchange–correlation functional and 6-311++ G (d, p) basis set. The Vibration frequency was calculated for optimized structure in the gas phase with the same level of theory. The DFT calculated vibrational frequencies are found to be higher than experimental vibration, to overcome this we scale the calculated frequencies by scaling factor 0.96

Table 1 Crystal data and structure refinement for the title compound

Crystal parameters	1
Empirical formula	$C_{16}H_{12}Cl_2O_2$
Formula weight	307.16
Temperature (K)	273(2)
Wavelength (Å)	1.54178
Crystal system	Orthorhombic
Space group	P 2_1 2_1 2_1
a (Å)	6.4704 (4)
b (Å)	12.9304 (8)
c (Å)	16.7181(11)
α (°)	90
β (°)	90
γ (°)	90
Volume ($Å^3$)	1398.72(15)
Z	4
$D_{Calc.}$ (Mg/m^3)	1.459
Absorption coefficient (mm^{-1})	4.156
F (000)	632
Crystal size (mm^3)	0.302 × 0.100 × 0.020
Theta ranges for data collection (°)	4.322 to 66.667
Index ranges	−6 ≤ h ≤ 7, −15 ≤ k ≤ 15, −19 ≤ l ≤ 19
Reflections collected	8850
Independent reflections	2382 [R (int.) = 0.0571]
Completeness to theta	66.667°,97.5%
Refinement method	Full-matrix least-squares on F^2
Data/restraints/parameters	2382/0/183
Goodness-of-fit on F^2	3.229
Final R indices [I > 2σ (I)]	R_1 = 0.1216, wR_2 = 0.1575
R indices (all data)	R_1 = 0.1230, wR_2 = 0.1577
Absolute structure parameter	0.164 (13)
Extinction coefficient	0.0017(14)
Largest diff. peak and hole, e.$Å^{-3}$	0.860 and −0.637

Scheme 1 The synthetic route of the title compound

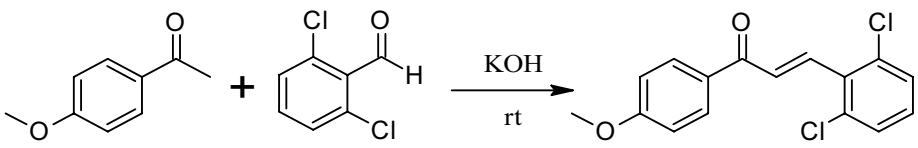

1 2 3

Table 2 Selected experimental and theoretical geometrical parameters of title compound

Bond[a]	Bond length [Å]		Bond[a]	Dihedral angle [°]	
	Experimental	Calculated		Experimental	Calculated
Cl(1)–C(9)	1.758(8)	1.7583	C(1)–O(1)–C(14)	117.8(6)	118
Cl(2)–C(00D)	1.746(8)	1.76	C(12)–C(4)–C(3)	118.4(7)	117.9
O(1)–C(1)	1.374(9)	1.3574	C(12)–C(4)–C(5)	123.2(7)	124.1
O(1)–C(14)	1.431(10)	1.4246	C(3)–C(4)–C(5)	118.3(7)	117.8
O(2)–C(5)	1.221(9)	1.2243	C(6)–C(7)–C(8)	128.0(9)	127.3
C(4)–C(12)	1.393(11)	1.4065	C(9)–C(8)–C(00D)	114.5(8)	115.3
C(4)–C(3)	1.394(10)	1.40	C(9)–C(8)–C(7)	119.4(8)	119.3
C(4)–C(5)	1.494(11)	1.401	C(00D)–C(8)–C(7)	125.9(8)	125.9
C(7)–C(6)	1.330(11)	1.3399	C(1)–C(2)–C(3)	119.8(8)	119.5
C(7)–C(8)	1.470(12)	1.4699	C(10)–C(11)–C(00D)	120.0(8)	119.8
C(8)–C(9)	1.398(11)	1.4125	C(7)–C(6)–C(5)	119.9(9)	119.8
C(8)–C(00D)	1.403(11)	1.411	O(2)–C(5)–C(6)	120.8(8)	120.6
C(2)–C(1)	1.378(11)	1.3574	O(2)–C(5)–C(4)	120.8(7)	120.5
C(2)–C(3)	1.389(10)	1.3885	C(6)–C(5)–C(4)	118.4(8)	118.9
C(11)–C(10)	1.374(10)	1.3847	C(2)–C(3)–C(4)	120.8(7)	121.6
C(11)–C(00D)	1.389(11)	1.3909	C(11)–C(00D)–C(8)	122.5(7)	122.4
C(6)–C(5)	1.495(11)	1.4927	C(11)–C(00D)–Cl(2)	116.3(6)	116.1
C(1)–C(13)	1.388(11)	1.4011	C(8)–C(00D)–Cl(2)	121.1(7)	121.3
C(10)–C(00J)	1.383(11)	1.39	C(2)–C(1)–O(1)	123.4(8)	124
C(12)–C(13)	1.381(10)	1.3846	C(2)–C(1)–C(13)	120.1(8)	115.3
C(00J)–C(9)	1.374(11)	1.3884	O(1)–C(1)–C(13)	116.5(7)	115.8
			C(11)–C(10)–C(00J)	119.9(8)	120.2
Torsional angle [°]	Experimental	Calculated	C(4)–C(12)–C(13)	120.9(7)	121.1
C(5)–C(6)–C(7)–C(8)	175(8)	178.8	C(1)–C(13)–C(12)	119.9(7)	120.15
			C(9)–C(00J)–C(10)	118.8(8)	119.22
			C(00J)–C(9)–C(8)	124.4(8)	123.1
			C(00J)–C(9)–Cl(1)	116.5(6)	117
			C(8)–C(9)–Cl(1)	119.2(7)	119.6

[a]Atom-numbering scheme Fig. 1a is used

[26] for better agreement with experimental values. None of the predicted vibrational frequencies has an imaginary frequency. The vibrational band assignments were made using the Gauss View 4.1.2 molecular visualization program [27]. The time-dependent density functional theory (TD-DFT) [28] was performed to obtain electronic absorption spectra at B3LYP/6-311++ G (d, p) level of theory in a vacuum of the optimized structure in the ground state. From Homo Lumo energies, global reactivity parameters were calculated with the help of the standard equation to investigate the reactivity and stability of the compound.

3 Results and discussion

3.1 Crystal structure and optimized structure analysis

The molecular crystal and optimized structure of the title compound are shown in Fig. 1a, b. This compound crystallizes in the orthorhombic crystal system of P-2_1 2_1 2_1 space group where the unit cell parameters are a = 6.4704 (4) Å, b = 12.9304 (8) Å, c = 16.7181 (11) Å, α = 90°, β = 90°, γ = 90° and Z = 4. The numbering of atom considered from the crystal structure (Fig. 1a). The methoxy substituted groups around the phenyl rings are almost planar. The molecular structure of the title compound (Fig. 1a) shows the methoxy substituent [O(1)] at the para position of one ring [C(1)–C(13)] and dichloro substituent atoms [Cl(1) and Cl(2)] at the ortho position of another ring [(C8)–C(00d)]. In the title compound, two aromatic rings exhibit non-planar geometry and it is due to the presence of two chlorine atoms on one phenyl ring. The selected geometrical parameters are listed in Table 2. The experimental C5–C6–C7–C8 torsion angle 175 (8)° and calculated observe at 178.8 (°), confirms the molecule exhibits an E configuration concerning the C6=C7 double bond. The presence of the α-β-unsaturated ketone is indicated by the shorter

experimental O2–C5 [1.221 (9) Å] and C6–C7 [1.330 (11) Å] bond lengths as seen in Table 2. The calculated O2–C5 and C6–C7 bond lengths are found to be 1.2243 Å and 1.3399 Å respectively for B3LYP. The experimental C–C bond length can be observed between 1.495 and 1.33 Å, calculated ones were between 1.4927 and 1.3399 Å (B3LYP). Experimental sp3 C–O bond length is observed between 1.4246 and 1.3574 Å, calculated ones were detected at 1.367–1.335 Å (B3LYP). The average C–Cl bond lengths of 1.732 Å and found within the expected range all bond lengths and angles are within the normal ranges and compared with previously reported structures of chalcones [29–31].

3.2 Mulliken atomic charges

Mulliken atomic charges calculated and reported in Table 3. Mulliken atomic charge calculation has an important role in the application of quantum chemical calculations to Molecular system because of atomic charge effects dipole moment, electronic structure and some other properties of the molecular system [32, 33]. As indicated in Table 3, the C_5 atom carries the largest positive charge (1.852333) among the other carbon atoms, therefore, expected to be the site for nucleophilic attack in the title compound. However, C_9 and C_{11} atoms carry the highest negative charge − 1.353074, − 1.240575, respectively amongst all carbon atoms. However, except hydrogen H_8 all hydrogen carries a positive charge.

Table 3 Mulliken atomic charges for title compound at B3LYP/6-311++ G (d, p) level

Atom	Charge	Atom	Charge
1 Cl	0.610822	17 C	0.037376
2 Cl	0.558039	18 H	0.191224
3 O	−0.147904	19 C	−0.623943
4 O	−0.233380	20 H	0.168847
5 C	1.852333	21 C	−0.319253
6 C	0.221456	22 H	0.155815
7 C	−0.232553	23 H	0.178752
8 H	−0.084901	24 H	0.155976
9 C	−1.353074	25 C	−0.336931
10 H	0.228569	26 C	−0.485683
11 C	−1.240575	27 H	0.215706
12 H	0.116248	28 C	0.322931
13 C	−0.005765	29 C	0.227336
14 C	−0.720658	30 H	0.203778
15 C	0.533903	31 C	−0.593436
16 H	0.194056	32 H	0.204888

3.3 FT-IR spectrum analysis

The FT-IR spectrum has been recorded in the region of 4000–500 cm^{-1} (solid phase) and the spectrum is shown in Fig. 2a. The calculated vibrational spectrum in the gas phase is shown in Fig. 2b. The molecule possesses C1 symmetric. There are 32 atoms in title molecule corresponding 90 fundamental modes of vibrations

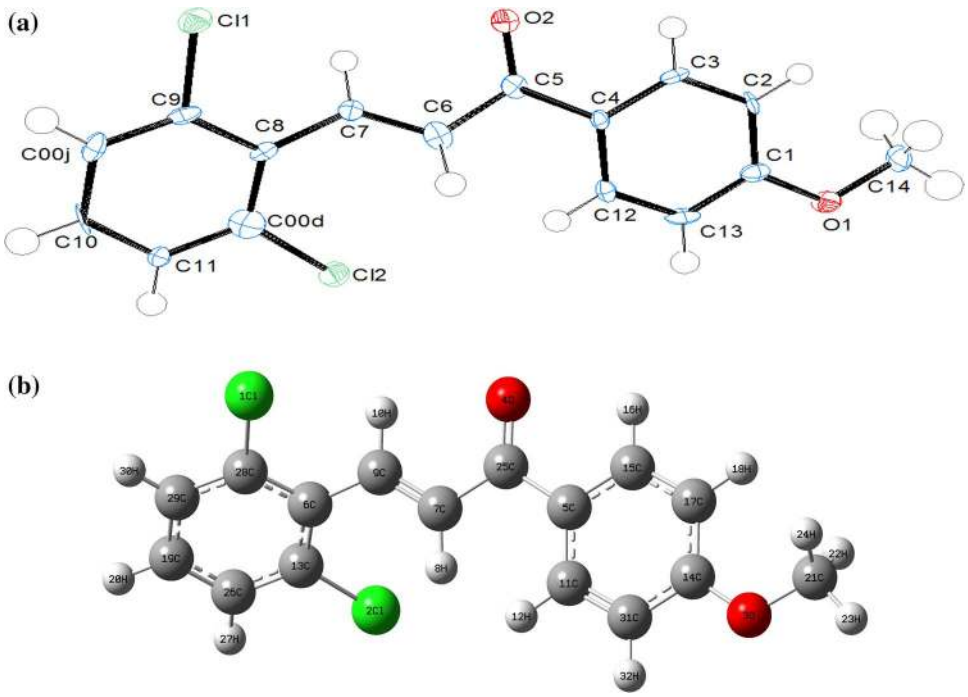

Fig. 1 **a** Molecular structure of the compound with a 50% ellipsoids probability with the atomic numbering scheme. **b** Optimized structure of (2E)-3-(2,6-dichlorophenyl)-1-(4-methoxyphenyl) prop-2-en-1-one

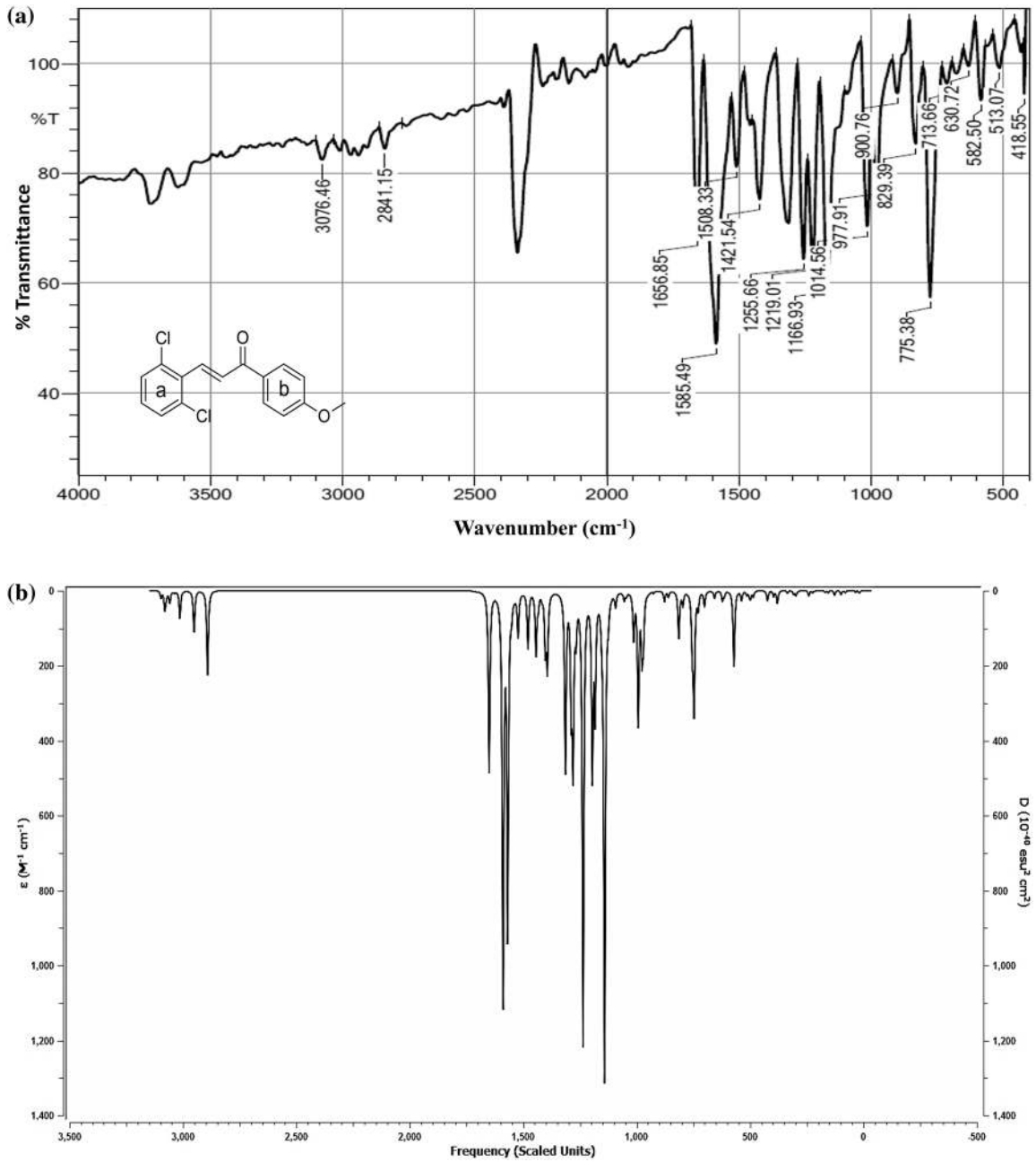

Fig. 2 **a** Experimental FT-IR spectrum of the title compound. **b** Simulated FT-IR spectrum of the title compound in the gas phase

calculated at B3LYP/6-311++ G (d, p) level. Some of the theoretical and experimental vibrations with intensity and their assignments are represented in Table 4. The carbonyl stretching vibrations in Chalcones generally appear in the region 1750–1600 cm^{-1} [29]. We assign carbonyl stretching, vibration in the experimental spectrum at 1656 cm^{-1} and theoretically at 1650 cm^{-1}. These values agree with previously reported values of Chalcones derivatives [30, 31]. The C-H stretching vibrations of aromatic and vinyl groups were normally seen in the region above 3000 cm^{-1} [34]. These vibrations are calculated in the range of 3097–3073 cm^{-1} and experimentally it observed at 3076 cm^{-1} as a mixed vibrational band. In-plane and out of plane C-H bending vibrations aromatic ring and vinyl group observe at 1255, 900, 829, 775 cm^{-1} (Table 4) and calculated at 1267, 877, 814, 790 cm^{-1}. In the previously reported literature on Chalcones derivatives stretching frequency of the C=C of enone, part was observed at 1592 cm^{-1} and calculated at 1588 cm^{-1} [30]. Here in the title molecule, this

Table 4 Selected experimental and theoretical vibrational assignment for the title compound calculated at B3LYP/6-311++ G (d, p) level

Selected mode no.	Calculated (scaled) frequencies in cm^{-1}	Calculated IR intensity	Experimental frequencies (cm^{-1})	Assignment
90	3097	5.21	–	ν_{sym} CH (Ring b) + ν_{sym} (7)C-(8)H (C=C)
89	3082	2.91	–	ν_{sym} CH (Ring a)
88	3080	11.88	–	ν_{sym} CH (Ring b)
87	3077	0.36	–	ν_{asym} CH (Ring a)
86	3073	3.21	3076	ν_{sym} CH (Ring b) + ν_{sym} (7)C(-8)H (C=C)
85	3065	0.17	–	ν_{asym} CH (Ring b)
84	3059	7.058	–	ν_{asym} CH (Ring b)
83	3056	2.72	–	ν_{asym} CH (Ring a)
82	3037	1.72	–	ν_{sym} (9)C-(10)H (C=C)
81	3013	20.93	–	ν_{asym} CH_3
80	2951	31.59	–	ν_{asym} CH_3
79	2891	64.93	2841	ν_{sym} CH_3
78	1650	138.98	1656	ν C=O
77	1589	313.86	1585	ν C=C
76	1568	260.98	–	ν C=C (Ring b)
75	1551	12.62	–	ν C=C (Ring a)
74	1537	1.33	–	ν C=C (Ring b)
73	1522	32.86	1508	ν C=C (Ring a)
72	1479	43.32	–	ν C=C (Ring b)
71	1443	47.89	–	CH_3 asym. def
70	1433	9.81	–	CH_3 asym. def
69	1417	3.70	1421	CH_3 sym. def
68	1402	43.10	–	CH_3 sym. def
67	1452	56.32	–	β CH (Ring a)
66	1389	4.34	–	β CH (Ring b)
65	1314	136.97	–	β CH (C=C)
62	1267	28.95	1255	β (7)C-(8)H (Ring b) + β CH (Ring b)
60	1236	346.34	1219	ν (14)C-(30)O
59	1195	136.47	1166	ν C–C
49	1013	34.97	1014	ν (30)O-(21)C
47	977	46.63	977	γ CH (C=C)
46	970	37.42	–	γ CH (ring b)
45	951	0.77	–	γ CH (ring a)
42	877	7.81	900	γ CH (C=C)
39	814	36.10	829	γ CH (ring b)
37	790	0.07	775	γ CH (ring b)
33	729	12.02	713	ν C-(1)Cl

v stretching, *asym* asymmetric, *sym* symmetric, *def* deformation, *β* in-plane bending, *γ* out of plane bending, *ρ* rocking, *Γ* torsion

vibration is computed at 1589 cm^{-1} and experimentally shown at 1585 cm^{-1}. The aromatic C=C stretching vibration for the title compound observed at 1508 cm^{-1} and theoretically assign at 1522 cm^{-1}. Out of plane bending vibration at 977 cm^{-1} indicates the Trans geometry of alkene. In the present study, C–Cl stretching vibrations were observed at 713 cm^{-1} and calculated at 729 cm^{-1}. The peaks due to asymmetric and symmetric methyl stretching modes commonly observed at 2965 and 2880 cm^{-1}

Table 5 The excitation energy (eV), oscillator strength, wavelength (nm) calculated using TD-DFT method in vacuum and experimental wavelength in dichloromethane solvent

Theoretical absorption λ (nm) (vacuum)	Experimental absorption λ (nm) (in dichloromethane)	𝔽 (oscillator strength) (vacuum)	Excitation energy (eV) (vacuum)
337	–	0.4422	3.6772
301	308	0.2468	4.1096

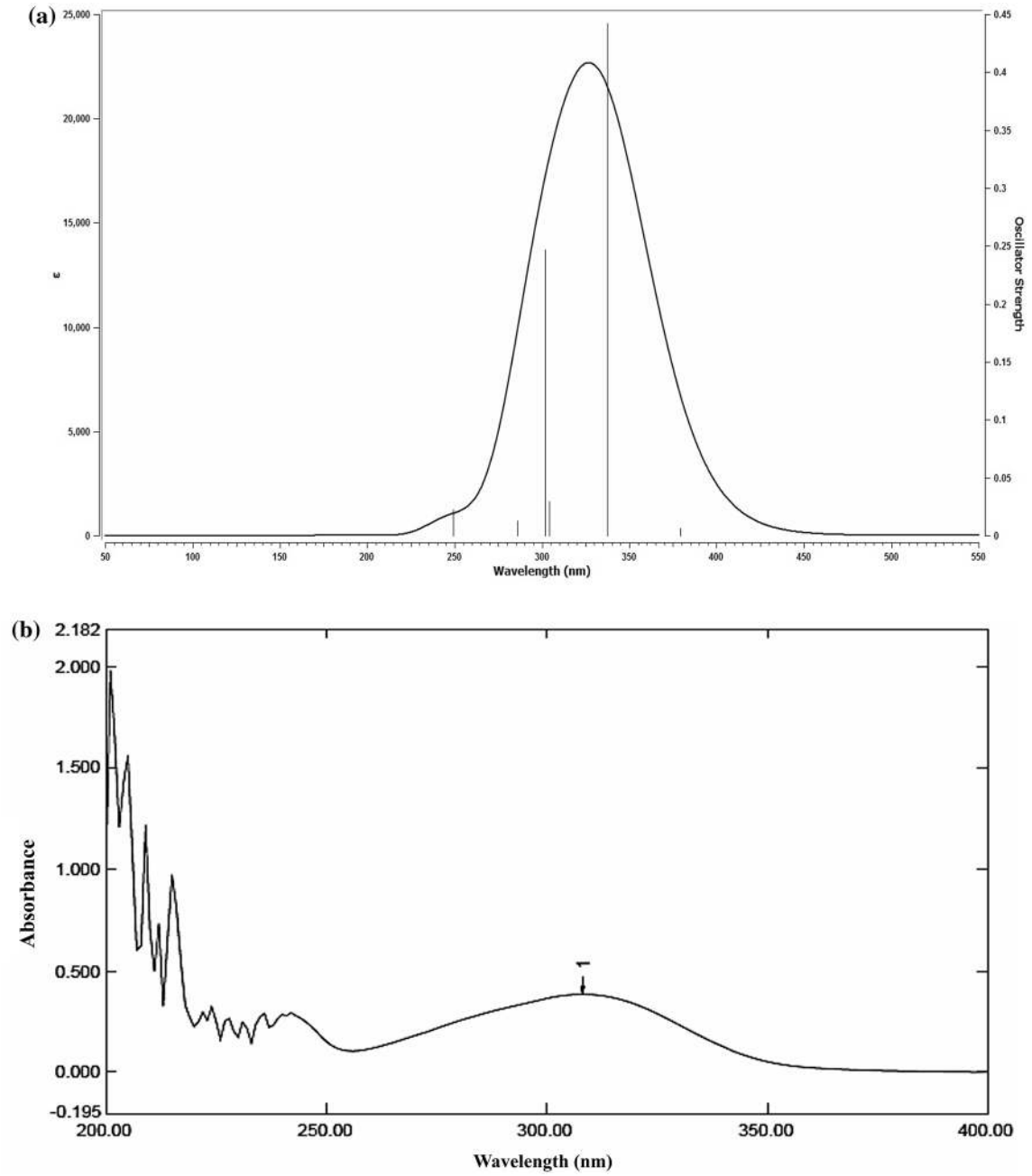

Fig. 3 **a** Simulated UV–visible absorption spectra for the title compound computed at B3LYP/6-311++ G (d, p) level of theory in vacuum. **b** The experimental UV–visible absorption spectra for the title compound in dichloromethane

[35]. The methyl group stretching vibrations calculated in the range of 3013–2891 cm^{-1} are shown in Table 4. In experimental FT-IR, symmetric stretching vibration mode of the methyl group is observed at 2841 cm^{-1}. Asymmetric and symmetric deformation of methyl group normally appears in the region of 1465–1440 cm^{-1} and 1390–1370 cm^{-1} respectively [36, 37]. In the present case methyl group deformation calculated at 1417 $cm^{-1}$and observe at 1421 cm^{-1}.

3.4 Electronic spectra analysis

The electronic transitions in the UV–visible spectrum of title compound have been studied by the time-dependent density functional theory (TD-DFT) where allowed transitions are calculated in the gas phase. The electronic absorption spectrum of title molecule recorded experimentally in dichloromethane (DCM) solvent. The calculated electronic transitions of high oscillatory strength,

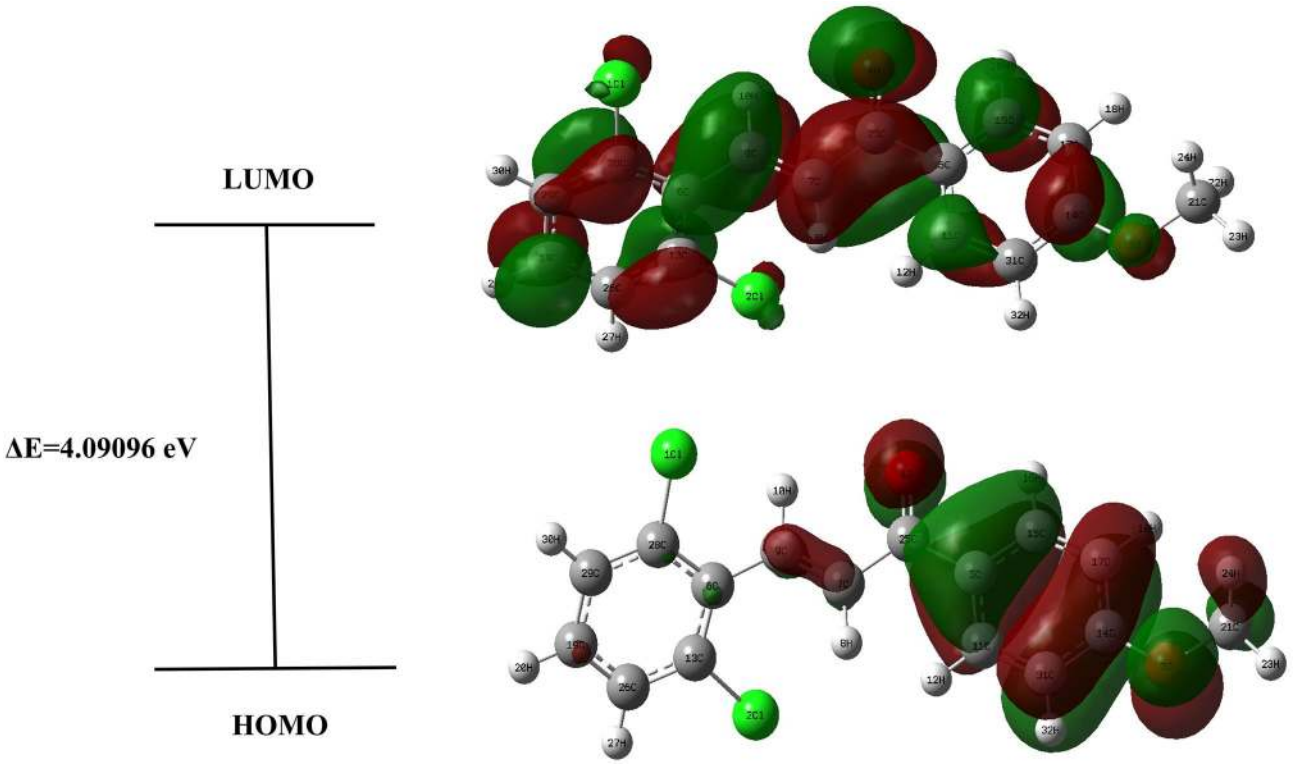

Fig. 4 The HOMO–LUMO plot of title compound obtained at B3LYP/6-311G++ (d, p) level

wavelength and experimentally determined wavelength are given in Table 5. Simulated spectrum is illustrated in Fig. 3a and experimental in Fig. 3b Computed UV–visible spectrum exhibited two intense allowed transitions at λ max = 337 nm, $f = 0.4422$ and λ = 301 nm, $f = 0.2468$. Which have corresponded to the experiment λ max value of 308 nm. The observed peak in theoretical spectra indicated redshift as compared with experimental ones, so the assigned bands were characterized by ($n \rightarrow \pi^*$) and ($\pi \rightarrow \pi^*$) transitions. In HOMO, a π bonding electron is spread over phenyl ring, carbonyl oxygen atom and C=C moiety. In LUMO, electrons it is spread to the entire molecule except for the methyl group.

Table 6 Global chemical reactivity indices for the title compound calculated at B3LYP/6-311G++ (d, p) level

Molecular properties	B3LYP/6-311++ G(d,p)
E_{LUMO} (eV)	− 2.466711
E_{HOMO} (eV)	− 6.55767
$\Delta E = E_{LUMO} - E_{HOMO}$ (eV)	4.09096
Electron affinity (A)	2.46671
Ionization energy (I)	6.55767
Global hardness (η)	2.04548
Chemical softness (S)	0.48888
Electronic chemical potential (μ)	− 4.51219
Global electrophilicity index (ω)	4.97654

3.5 HOMO–LUMO and global chemical reactivity descriptor

The highest occupied molecular orbital (HOMO) and the lowest occupied molecular orbital (LUMO) are called Frontier molecular orbitals (FMOs). The HOMO, LUMO energy value and energy gap values for title compound were computed at TD-DFT/ B3LYP/6-311++ G (d, p) level of theory in the gas phase. The HOMO–LUMO Plot for the title compound in the gas phase is shown in Fig. 4. The HOMO represents the ability to donate electrons, whereas LUMO as an electron acceptor [38]. The computed gas phase HOMO and LUMO energies are − 6.55767 eV and − 2.466711 eV respectively, whereas the energy gap is found 4.09096 eV. The quantum chemical parameters such as ionization potential (I), electron affinity (A), chemical hardness (η), chemical softness (S), electronic chemical potential (μ), global electrophilicity index (ω), are used to predict the reactivity and stability of the compound. On the basis of Koopman's theorem [39], all these parameters were calculated from HOMO–LUMO energy using Eqs. 1–4 [40–43].

$$\eta = {}^{1}/_{2}(I-A) \quad (1)$$

Table 7 Antimicrobial activity of synthesized compound

Product	Bacteria				Fungi		
	Ec	*Bs*	*St*	*Sa*	*An*	*Af*	*Ca*
Compound	08 (25)	11 (25)	08 (50)	07 (50)	13 (25)	10 (25)	10 (25)
Penicillin	15 (25)	17 (25)	13 (25)	13 (25)	NA	NA	NA
Nystatin	NA	NA	NA	NA	16 (25)	14 (25)	13 (25)

Zone of inhibition expressed in mm, MIC values (mg/mL) is given in brackets, MIC > 50 mg L^{-1}, DMSO and water as the solvent

Ec Escherichia coli, Bs Bacillus subtillis, Sa Staphylococcus aureus, St Salmonella typhi, An Aspergillus niger, Af Aspergillus flavus, Ca Candida albicans

$$S = 1/\eta \quad (2)$$

$$\mu = -{}^{1}/_{2}(I + A) \quad (3)$$

$$\omega = \mu^2/2\eta \quad (4)$$

where I and A are ionization potential and electron affinity of the compound respectively ($I = -\varepsilon_{HOMO}$) and ($A = -\varepsilon_{LUMO}$). The HOMO, LUMO energies and global reactivity parameters are listed in Table 6. From the calculation, it was found that the title compound is kinetically stable with the hardness value of 2.04548 eV. The chemical softness of 0.488 eV, the chemical potential of −4.51219 eV and the electrophilicity index of 4.97654 eV suggest that title compound possesses excellent chemical strength and stability.

3.6 Antimicrobial activities of the synthesized compound

The newly synthesized compound (2E)-3-(2,6-dichlorophenyl)-1-(4-methoxyphenyl) prop-2-en-1-one were screened for their antimicrobial activities in vitro against *Staphylococcus aureus, Bacillus subtillis, Escherichia coli* and *Salmonella Typhi* Pathogenic bacteria and three fungi *Aspergillus Niger, Aspergillus flavus, Candida albicans*. The activities of the titled compound were tested using the agar diffusion method [44]. The antibiotic Penicillin (25 µg/mL) used as a reference drug for antibacterial activity and Nystatin (25 µg/mL) for antifungal activities. The dimethyl sulphoxide (1% DMSO) was used a control without compound.

The culture strains of bacteria were maintained on a nutrient agar slant at 37 ± 0.5 °C for 24 h. The antibacterial activity was evaluated using nutrient agar plate seeded with 0.1 mL of respective bacterial culture stain suspension Prepared in sterile saline (0.85%) of 10^5 CFU/mL dilution. The well of 6 mm diameter was filled with 0.1 mL of a compound solution of concentration 25 to 150 µg/mL separately for each bacterial strain. All the plates were incubated at 37 ± 0.5 °C for 24 h. The zone of inhibition of compound in mm was noted and minimum inhibitory concentration (MICs) was noted.

For antifungal activity, all the culture strains of fungi maintain on potato dextrose agar (PDA) slant at 27 ± 0.2 for 24–48 h till sporulation. Spores of strains were transferred into 5 mL of sterile distilled water containing 1% Tween-80 (to suspend the spore properly). The spores were counted by haemocytometer (10^6 CFU/mL). The sterile PDA plate was prepared to contain 2% agar, 0.1 mL of each fungal spore suspension was spread on each plate and incubated at 27 ± 0.2 °C for 12 h. After incubation well prepared using sterile cork borer and each agar well was filled with 0.1 mL of compound solution at concentration 25 to 150 µg/mL. The Plates were kept in the refrigerator for 20 min for diffusion and then incubated at 27 ± 0.2 °C for 24–28 h. After incubation, the zone of inhibition of the compound was measured in mm along with standard and minimum inhibitory concentration (MICs) were noted.

The results of antimicrobial activity are given in Table 7. From the result of antimicrobial data, the compound was found moderately active against bacteria *Subtillis*, *E. coli*. The Compound does not show promising activity against all other Bacteria. The compound also exhibits moderate activity against all fungi as compared to standard.

4 Conclusion

The title compound (2E)-3-(2,6-dichlorophenyl)-1-(4-methoxyphenyl)prop-2-en-1-one has been synthesized and characterized by IR, HR-MS, ^{1}H NMR method. Its three-dimensional structure was obtained by single-crystal XRD. The experimental and theoretical study confirmed that the molecule exhibits an E configuration. Theoretically calculated bond length, bond angle and λ_{max} (UV spectrum) show good agreement with experimental results. The HOMO–LUMO energy gap is in good agreement with experimental results. FT-IR spectra of the title molecule show good correlation with theoretically assigned vibrational modes. The electronic spectral properties of

the studied compound were calculated by the TD-DFT method. The chemical reactivity parameters indicate that the title compound possesses excellent chemical strength and stability. The compounds exhibited moderate antimicrobial activity against bacteria *B*. *Subtillis*, *E. coli* and all tested fungus as compared with their standards used.

5 Supplementary information

Crystallographic data are available on htttp://www.ccdc.cam.ac.uk upon request quoting deposition number CCDC 1988019 for the (2E)-3-(2, 6-dichlorophenyl)-1-(4-methoxyphenyl)-prop-2-en-1-one.

Acknowledgements The authors acknowledge Central Instrumentation Facility, Savitribai Phule Pune University, Pune for providing a necessary facility for carrying out the XRD and other spectral analysis. Nutan Sadgir is also thankful to the University Grant Commission (UGC) for minor research project (F- 47-1125/14 (General /87/WRO), New Delhi for a financial assistant to carry out the research work.

Compliance with ethical standards

Conflict of interest The authors declare that they have no conflict of interests.

References

1. Rane RA, Telekar VN (2010) Synthesis and evaluation of novel chloropyrrole molecules designed by molecular hybridization of common pharmacophores as potential antimicrobial agents. Bioorg Med Chem Lett 20(19):5681–5685
2. Nielsen SF, Bosen T, Larsen M, Schonning K, Kromann H (2004) Antibacterial chalcones—bioisosteric replacement of the 4-hydroxy group. Bioorg Med Chem 12(11):3047–3054
3. Zheng Y, Wang X, Gao S, Ma Min, Ren G, Liu H, Chen X (2015) Synthesis and antifungal activity of chalcone derivatives. Nat Prod Res 29(19):1804–1810
4. Edenharder R, Petersdorff IV, Rauscher R (1993) Antimutagenic effects of flavonoids, chalcones and structurally related compounds on the activity of 2-amino-3-methylinidazo [4,5-*f*] quinoline (IQ) and other heterocyclic amine mutagens from cooked food. Mutat Res 287(2):261–274
5. Boumendjel A, Boccard J, Carrupt PA, Nicolle E, Blanc M, Geze A, Choisnard L, Wouessidjewe D, Matera EL, Dumontet C (2008) Antimitotic and antiproliferative activities of chalcones: forward structure-activity relationship. J Med Chem 51(7):2307–2310
6. Kumar D, Kumar NM, Akamatsu K, Kusaka E, Harada H, Ito T (2010) Synthesis and biological evaluation of indolyl chalcones as antitumor agents. Boorg Med Chem Lett 20(19):3916–3919
7. Sivakumar PM, Prabhakar PK, Doble M (2011) Synthesis, antioxidant evaluation, and quantitative structure-activity relationship studies of chalcones. Med Chem Res 20(4):480–492
8. Nowakowska Z (2007) A review of anti-infective and anti-inflammatory chalcones. Eur J Med Chem 42(2):125–137
9. Yadav N, Dixit SK, Bhattacharya A, Mishra LC, Sharma M, Awasthi SK, Bhasin VK (2012) Antimalarial activity of newly synthesized chalcone derivatives in vitro. Chem Biol Drug Des 80:340–347
10. Liu M, Wilairat P, Croft SL, Tan AL, Go ML (2003) Structure–activity relationships of antileishmanial and antimalarial chalcones. Bioorg Med Chem 11(13):2729–2738
11. Gomes MN, Braga RC, Grzelak EM, Neves BJ, Muratov E, Ma R, Klien LL, Cho S, Oliveira GR, Franzblau SH, Andrade CH (2017) QSAR-driven design, synthesis and discovery of potent chalcone derivatives with antitubercular activity. Eur J Med Chem 137:126–138
12. Hsieh CT, Hsieh TJ, El-Shazly M, Chuang DW, Tsai YH, Yen CT, Wu SF, Wu YC, Chang FR (2012) Synthesis of chalcone derivatives as potential anti-diabetic agents. Bioorg Med Chem Lett 22(12):3912–3915
13. Almeida JR, Moreira J, Pereira D, Pereira S, Antunes J, Palmeira A, Vasconcelos V, Pinto M, Correia-da-Silva M, Cidade H (2018) Potential of synthetic chalcone derivatives to prevent marine biofouling. Sci Total Environ 643:98–106
14. Krawczyk P, Czeleń P, Szefler B, Cysewski P (2017) Theoretical studies on the interaction between chalcone dyes and Concanavalin A-the reactive group effects on the photophysical and biological properties of the fluorescence probe. J Photochem Photobiol A 346:327–337
15. Makhlouf MM, Radwan AS, Ghazal B (2018) Experimental and DFT insights into molecular structure and optical properties of new chalcones as promising photosensitizers towards solar cell applications. Appl Surf Sci 452:337–351
16. Leory K, George EI, Melville H, Basil D, Ricagrd W, Richard R (1968) Dihydrochalcones. Synthesis of potential sweetening agents. J Agric Food Chem 16(1):108–112
17. Sarojini BK, Narayana B, Ashalath BV, Indira J, Lobo KG (2006) Synthesis, crystal growth and studies on the non-linear optical property of new chalcones. J Cryst Growth 295(1):54–59
18. Coskun D, Gunduz B, Coskun MF (2019) Synthesis, characterization and significant optoelectronic parameters of 1-(7-methoxy-1-benzofuran-2-yl) substituted chalcone derivatives. J Mol Struct 1178:261–267
19. Delavaux-Nicot B, Maynadie J, Lavabre D, Fery-Forgues S (2007) Ca2+ *vs*. Ba2+ electrochemical detection by two disubstituted ferrocenyl chalcone chemosensors. Study of the ligand–metal interactions in CH_3CN. J Organomet Chem 692(4):874–886
20. Lu Z, Zhang F, Lei X, Yang XuS, Duan X (2008) In situ growth of layered double hydroxide films on anodic aluminium oxide/aluminium and its catalytic feature in aldol condensation of acetone. Chem Eng Sci 63(16):4055–4062
21. Sheldrick GM (1997) SHELXL97, a program for the refinement of crystal structures. University of Göttingen, Göttingen
22. Farrugia LJ (1997) ORTEP-3 for Windows—a version of ORTEP-III with a graphical user interface. J Appl Cryst 30:565
23. Frisch MJ, Trucks GW, Schlegel HB, Scuseria GE, Robb MA, Cheeseman JR, Montgomery JA Jr, Vreven T, Kudin KN, Burant JC, Millam JM, Iyengar SS, Tomasi J, Barone V, Mennucci B, Cossi M, Scalmani G, Rega N, Petersson GA, Nakatsuji H, Hada M, Ehara M, Toyota K, Fukuda R, Hasegawa J, Ishida M, Nakajima T, Honda Y, Kitao O, Nakai H, Klene M, Li X, Knox JE, Hratchian HP, Cross JB, Adamo C, Jaramillo J, Gomperts R, Stratmann RE, Yazyev O, Austin AJ, Cammi R, Pomelli C, Ochterski JW, Ayala PY, Morokuma K, Voth GA, Salvador P, Dannenberg JJ, Zakrzewski VG, Dapprich S, Daniels AD, Strain MC, Farkas O, Malick DK, Rabuck AD, Raghavachari K, Foresman JB, Ortiz JV, Cui Q, Baboul AG, Clifford S, Cioslowski J, Stefanov BB, Liu G, Liashenko A, Piskorz P, Komaromi I, Martin RL, Fox DJ, Keith T, Al-Laham MA, Peng CY, Nanayakkara A, Challacombe M, Gill PMW, Johnson B, Chen W, Wong MW, Gonzalez C, Pople JA (2003) Gaussian 03, Revision B.03. Gaussian, Inc., Pittsburgh, PA

24. Becke AD (1993) Density-functional thermochemistry III the role of exact exchange. J Chem Phys 98(7):5648–5652
25. Lee C, Yang W, Parr RG (1988) Development of Colle–Salvetti correlation-energy formula into a functions of the electron density. Phys Rev B 37(2):785
26. Sundaraganesan N, Elango G, Sebastian S, Subramani P (2009) Molecular structure, vibrational spectroscopic studies and analysis of 2-fluoro-5-methylbenzonitrile. Ind J Pure Appl Phys 47(7):481–490
27. Dennington R, Keith T, Millam J (2007) Gauss view, version 4.1.2. Semichem Inc., Shawnee Mission, KS
28. Runge E, Gross EKU (1984) Density-functional theory for time dependent system. Phys Rev Lett 52(12):997–1000
29. Roeges NPG (1994) A guide to the complete interpretation of infrared spectra of organic structures. Wiley, New York
30. Zainuri DA, Arshad S, Khalib CN, Razak IA, Pillai RR, Sulaiman SF, Hashim NS, Ooi KL, Armakovic S, Armakovic SJ, Panicker CY, Alsenoy CV (2017) Synthesis, XRD crystal structure, spectroscopic characterization (FT-IR, 1H and 13C NMR), DFT studies, chemical reactivity and bond dissociation energy studies using molecular dynamics simulations and evaluation of antimicrobial and antioxidant activities of a novel chalcone derivative, (E)-1-(4-bromophenyl)-3-(4-iodophenyl)prop-2-en-1-one. J Mol Struct 1128:520–533
31. Maidur SR, Patil PS, Ekbote A, Chia TS, Quah CK (2017) Molecular structure, second and third-order nonlinear optical properties and DFT studies of a novel non-centrosymmetric chalcone derivative: (2E)-3-(4-fluorophenyl)-1-(4-{[(1E)-(4-fluorophenyl) methylene]amino}phenyl)prop-2-en-1-one. Spectrochim Acta Part A Mol Biomol Spectrosc 184:342–354
32. Govindrajan M, Karabacak M, Savitha A, Periandy S (2012) FT-IR, FT-Raman, ab-initio HF and DFT study, NBO, HOMO–LUMO and electronic structure calculation on 4-chloro-3-nitrotolune. Spectrochima Acta Part A 89:137–148
33. Gunasekaran S, Kumaresan S, Arunbalaji R, Anand G, Srinivasan S (2008) Density functional theory study of vibrational spectra and assignment of fundamental modes of dacarbazine. J Chem Sci 120(3):315–324
34. Varsanyi G (1974) Assignments of the spectra of 700 benzene derivative. Academic Press, New York
35. Colthup NB, Daly LH, Wimberly SE (1990) Introduction to infrared & Raman spectroscopy. Academic Press, New York
36. Dhonnar SL, Jagdale BS, Sawant AB, Pawar TB, Chobe SS (2016) Molecular structure, vibrational spectra and theortical HOMO–LUMO analysis of (E)-3,5-dimethyl-1-phenyl-4-(p-tolyldiazenyl)-1H-pyrazole by DFT method. Der Pharma Chem 8(17):119–128
37. Arshad S, Zainuri DA, Khalib NC, Thanigaimani K, Rosil MM, Razak IA, Sulaiman SF, Hashim NS, Ooi KL (2018) Structure, spectroscopic properties and theoretical studies of (E) -1-(4-bromophenyl) -3-(2,3,4-trimethoxyphenyl) prop-2-en-1-one as a potential anti-oxidant agent. Mol Cryst Liq Cryst 664(1):218–240
38. Mishra R, Srivastava A, Sharma A, Tondon P, Baraldi C, Gameroni MC (2013) Structural, electronic, thermodynamical and charge transfer properties of chlorophenicol palmitate using vibrational spectroscopy and DFT calculations. Spectrapchemica Acta Part A Mol Biomed Spectrosc 101:335–342
39. Koopmans TA (1934) On the assignment of wave functions and Eigen energies to the individual electrons of an atom. Physica 1:104–133
40. Pearson RG (1989) Absolute electronegativity and hardness: application to organic chemistry. J Org Chem 54:1423–1430
41. Parr RG, Sznetpaly LV, Liu SJ (1999) Electrophilicity index. J Am Chem Soc 121:1922–1924
42. Chattaraj PK, Giri S (2007) Stability reactivity and aromaticity of compound of multivalent superatom. J Phys Chem A 111:11116–11126
43. Chattaraj PK, Maiti Sarkar U (2003) Philicity: a unified treatment of chemical reactivity and selectivity. J Phys Chem A 107:1089–5639
44. Shrinivasan D, Sangeetha N, Suresh T, Lakshamanperumalsamy P (2001) Antimicrobial activity of certain Indian medicinal plants used folkloric medicines. J Ethnopharmacol 74:217–220

Publisher's Note Springer Nature remains neutral with regard to jurisdictional claims in published maps and institutional affiliations.